Overview of the ISS radiation environment observed during the ESA EXPOSE-R2 mission in 2014-2016

T.P. Dachev[1], N.G. Bankov[1], B. T. Tomov[1], Yu. N. Matviichuk[1], Pl. G. Dimitrov[1], D.-P. Häder[2], G. Horneck[3]

[1]Space Research and Technology Institute, Bulgarian Academy of Sciences, Sofia, Bulgaria.

[2]Friedrich-Alexander Universität Erlangen-Nürnberg, Dept. Biology, Neue Str. 9, 91096 Möhrendorf, Germany

[3]DLR, Institute of Aerospace Medicine, Köln, Germany

Corresponding author: Tsvetan Dachev (tdachev59@gmail.com)

Key Points:

- A new radiation source selection procedure was implemented and verified using the shapes of the deposited energy spectra;

- Four radiation sources (including SEP) at locations around the ISS are identified and analyzed;

- The average equivalent skin and eyes doses for 30 days and 1 year calculated by R3DR2 are much smaller than the radiation protection guidance for LEO (NCRP, Report 132);

Abstract

The radiation risk radiometer-dosimeter (R3D)-R2 solid-state detector performed radiation measurements at the European Space Agency EXPOSE-R2 platform outside of the Russian "Zvezda" module at the International Space Station (ISS) from 24 October 2014-11 January 2016. The ISS orbital parameters were: average altitude of 415 km and 51.6° inclination. We developed special software and used experimentally-obtained formulas to determine the radiation flux-to-dose ratio from the R3DR2 Liulin-type deposited-energy spectrometer. We provide for the first time simultaneous, long-term estimates of radiation dose external to the ISS for four source categories: (i) galactic cosmic ray particles and their secondary products; (ii) protons in the South Atlantic Anomaly region of the inner radiation belt (IRB); (iii) relativistic electrons and/or bremsstrahlung in the outer radiation belt (ORB); and (iv) solar energetic particle (SEP) events. The latter category is new in this study. Additionally, in this study, secondary particles (SP) resulting from energetic particle interaction with the detector and nearby materials are identified. These are observed continuously at high latitudes. The detected SPs are identified using the same sorting requirements as SEP protons. The IRB protons provide the highest consistent hourly dose, while the ORB electrons and SEPs provide the most extreme hourly doses. SEPs were observed 11 times during the study interval. The R3DR2 data support calculation of average equivalent doses. The 30-day and 1-year average equivalent doses are much smaller than the skin and eyes doses recommendations by the National Council on Radiation Protection (Report 132), which provides radiation protection guidance for Low Earth Orbit.

1 Introduction and Motivation

Multiple space radiation experiments have been conducted at the International Space Station (ISS) and on other Low Earth Orbiting (LEO) platforms (Dachev et al., 2002; Reitz et al., 2005; Nealy et al., 2007; Wilson et al., 2007; Slaba et al., 2011, Badavi, 2014). As noted in Dachev et al. (2016a) during the past 16 years numerous ionizing radiation instruments have successfully flown on the ISS and European Space Agency's (ESA) Biopan-5/6 facilities on Foton M2/M3 satellites (Häder et al., 2009; Damasso et al., 2009). Recently ESA's EXPOSE multi-use platform has performed three experiments, designated as E, R and R2, all of which hosted the deposited energy spectrometer (DES) radiation risk radiometer-dosimeter (R3D) instruments (Dachev et al., 2012a; 2012b; 2015b; Schuster et al., 2012). These detectors were collaboratively developed by Bulgarian and German teams (Häder and Dachev 2003; Häder et al., 2009) and have been part of a suite of astrobiology instruments (Rabbow et al., 2012, 2015 and de Vera et al., 2012). Figure 1 shows an external view of the radiation risk radiometer-dosimeter (R3D)-R2 (R3DR2) instrument mounted on the EXPOSE-R2 facility. The current R3DR2 spectrometer-dosimeter onboard the ISS is the same instrument as flown in the EXPOSE-R facility from 2009-2010, which was called R3DR, but here is given the extension R2 to distinguish between the data from the previous mission.

Cucinotta et al. (2003) wrote: "The International space station provides significant challenges for radiation protection of the crew due to a combination of circumstances including: the extended duration of missions for many crewmembers, the exceptionally dynamic nature of the radiation environment in ISS orbit, and the necessity for numerous planned extravehicular activities (EVA) for station construction and maintenance. Radiation protection requires accurate radiation dose measurements and precise risk modeling of the transmission of high fluxes of energetic electrons and protons through the relatively thin shielding provided by the space suits worn during EVA." The citation above guides and

motivates us to present "accurate" radiation dose measurements made by the R3DR2 detector outside of the ISS Russian "Zvezda" module.

In this paper, we consolidate results from these previous papers and report on simultaneous radiation observations for four primary radiation sources, along with secondary protons, neutrons and heavier than H^+ ions (secondary particles (SP)) generated in the R3DR2 detector or nearby). Some of the results obtained during previous R3D experiments at the ISS are discussed in the remainder of this section and listed in Table 1. Preliminary information about the observed cosmic radiation time profile during the EXPOSE-R2 mission was published by Dachev et al. (2017).

These measurements provide depth-dose data for dosimetric support for other passive scientific experiments. The detector's shielding characteristics of 0.3 g cm^{-2} are very similar to the astronaut's space suits shielding (Benton et al., 2006). These data can be used for "precise risk modeling of the transmission of high fluxes of energetic electrons and protons through the relatively thin shielding provided by the space suits worn during EVA," (Cucinotta et al., 2003). Data can be used for future station module design also.

1.1 Galactic Cosmic Rays (GCR)

GCRs are a significant radiation component in the near-Earth and free-space environment consisting of 98% nuclei and 2% electrons. These energetic charged particles originate from sources beyond the solar system and convey energy ranging from several keV/nucleon up to 10^{12} MeV/nucleon. While most of the nuclei are protons (~87%) and alpha particles (~12%), heavier nuclei contribute ~1% (Simpson, 1983). The latter are typically referred to as high Z (HZ) and energy (HZE) particles, where Z is the atomic number. HZ particles play a particularly important role in space dosimetry (Horneck, 1994; Benton and Benton, 2001). The GCR component at the ISS altitudes vary slowly with solar activity. The average daily GCR dose rate observed by R3DR2 was 71.6 μGy d^{-1}. With similar solar modulation during the current epoch and the 2004 epoch (Potgieter, 2013), the EXPOSE-R2 mission GCR daily dose rate are similar to the DOSTEL dose rates in 2004 (Labrenz et al., 2015) of 77.6 μGy d^{-1}.

1.2 Trapped Radiation Belt Particles

High-energy charged particles are trapped by the Earth's magnetic field and form two distinct belts of toroidal shapes surrounding the Earth: the Inner Radiation Belt (IRB) and the Outer Radiation Belt (ORB).

The IRB is situated at an altitude from 0.2-2.0 Earth radii at the geomagnetic equator and consists of electrons, with energies of up to 10 MeV, and protons with energies of up to 700 MeV. As shown in Table 1 outside of the ISS, the IRB energetic protons deliver a daily dose of 567 μGy d^{-1}. During an analysis of the R3DE and R3DR data Dachev et al. (2011) discovered that the US Space Shuttle dockings with ISS decreased the dose rate from IRB 30-150 MeV proton fluxes. The effect was attributed to the additional shielding provided by the 78-ton Space Shuttle.

The ORB is located in the altitudinal range from 3.4-10 Earth radii. The ORB energetic population is electrons with energies of a few MeV. The first observations of the ORB relativistic electron fluxes in the ISS laboratory module were made in 2001 with a Liulin-E094 instrument (Dachev et al., 2002; Reitz et al., 2005). Later, ORB relativistic electron fluxes were observed with Liulin DES type instruments flown on the ISS and LEO satellites (Dachev et al., 2009b; 2012a; 2012b; 2015a, 2015b; 2016a). The ORB daily dose rate was 278 μGy d^{-1}. On quiet days the daily dose rate was practically zero, but reached

maximum dose rates up to 3000 µGy d^{-1} in the disturbed periods after magnetic storms. Extreme hourly values were 28,840 µGy h^{-1}.

1.3 Solar Energetic Particles

Solar flares and coronal mass ejections, caused by sporadic eruptions in the chromosphere and corona of the Sun, produce high fluxes of charged solar energetic particles (SEP) with energies up to several GeV. Historically the SEP measurements inside the ISS are rare, but have been discussed in Reitz et al., 2005; Larosa, et al., 2011; Di Fino et al., 2014; and Narici et al., 2015. Characteristics of SEP radiation dose were measured from September-October of 1989 inside the Russian space station "MIR" with the first Liulin type instrument (Petrov et al., 1994; Smart et al., 1994; Shurshakov et al., 1999) and with the Liulin-5 dosimetric telescope (DT) inside the ISS in March 2012 (Semkova et al., 2014). With the R3DR2 instrument, we performed one of the first SEP measurements outside of the ISS (Dachev et al., 2016a). The highest SEP hourly dose rate measured during the EXPOSE-R2 mission was 5251 µGy h^{-1} on 22 June 2015.

1.4 Secondary Particle radiation

Secondary radiations produced by the interactions of primary GCR and IRB protons with spacecraft materials and detectors are an important, and sometimes dominant, radiation environment for sensitive scientific instruments and biological systems (Dyer et al., 1996). Neutrons are the major component of secondary radiation followed by protons and other lighter particles.

Previous simultaneous measurements outside of the ISS (Dachev, 2013) suggest that the EXPOSE-E facility (R3DE) instrument was heavily shielded by surrounding materials of the European Technology Exposure Facility, producing a daily average dose rates of 93 µGy d^{-1} from 12 March – 20 June 2009. The less shielded radiometer-dosimeter R3DR instrument that was mounted outside the Russian "Zvezda" module of the ISS, (physically the same as the R3DR2 discussed here) yielded only 85 µGy d^{-1} during the same period. The higher dose rates measured with a higher shielded R3DE instrument were explained as additional dose from secondary particles in the shielding materials. The estimations of the GCR exposure behind different shielding by Mrigakshi et al. (2013) confirmed these results and the importance of the secondary radiation. The secondary particles delivered a daily dose rate to the R3DR2 instrument of a few µGy d^{-1}.

2 Materials and Methods-- R3DR2 Instrument Description

Figure 1 shows an external view of the R3DR2 instrument mounted on the EXPOSE-R2 facility. The R3DR2 instrument is a small-dimension (76x76x36 mm), low-mass (0.17 kg) automatic device that measures solar electromagnetic radiation in four channels and ionizing radiation in 256 channels of a Liulin-type DES (Dachev et al., 2015a). In Fig. 1 small circles on the surface in the central portion of the R3DR2 instrument show the four solar visible-and UV-radiation photodiodes, whose data are not addressed in this paper. The ionizing radiation detector (silicon PIN diode of Hamamatsu S2744-08 type) is located behind the aluminum wall of the instrument and is therefore not visible.

The ionizing radiation is monitored using a Hamamatsu silicon PIN diode detector, with 2 cm^2 area and 0.03 cm thickness (Fig. 2 (Dachev et al., 2012a)). After passing a charge-sensitive preamplifier, the signal is digitized by a 12-bit fast analog to digital (A/D) converter. The doses (deposited energies) are determined by a pulse height analysis technique and then passed to a discriminator. The pulse amplitudes, A[V], are transformed into digital

signals, which are sorted into 256 channels by a multi-channel analyzer. For every exposure interval of 10-s, a single energy deposition spectrum is collected. The energy channel number 256 accumulates all pulses with amplitudes exceeding the maximal level of the spectrometer of 20.83 MeV. All pulses in the 256th channel were considered to be equal to the minimum energy level for this channel and were added to the dose calculation. Using statistics of about 2.5 million 10-s data points from R3DE instrument, flown in 2008-2009 on ISS, we found that on average 1 event in the 256th channel occurred once per 6.2 hours of measurements. Dachev (2009a) describes the methods for characterizing the incoming space radiation.

A system international (SI) determination of the dose was used to calculate the absorbed dose in the silicon detector. The SI dose is the energy in Joules deposited in one kilogram of matter. The following equation relates the dose to energy loss and detector mass:

$$D(Gy) = \sum_{i=1}^{255} N_i E_i M D^{-1}$$

(1)

where *MD* is the mass of the detector in kg, N_i is the number of pulses registered in channel "i", E_i is the deposited energy (in Joules, known through the calibration of the detector) corresponding to channel "i".

The calibration procedures, which were performed with analogical R3DR2 instruments, are described in (Dachev et al., 2015a). The response curve of the R3DR2 instrument is expected to be very similar to that published by Uchihori et al. (2002) because all Liulin DES instruments were manufactured using same electronic parts and schematic. In the specific example of the calibration performed by Dr. Yukio Uchihori, it was found that the linear coefficient of the response curve, obtained during the calibrations with protons, He^{+} and Ne[+] ions, was equal to 81.3 keV, whereas the Liulin DES instruments predicted 81.4 keV. During the calibration process of the new Liulin DES type instruments, we adjusted the position of the first spectrometric channel using a [241]Am 60 keV gamma line. Furthermore, the linearity was controlled by electronic methods, as described by AMPTEK INC. in the A225 preamplifier operating notes (http://www.amptek.com/pdf/a225.pdf).

During the calibrations of Liulin type instruments it was found that the absolute values of the measured doses were within 2.8% and 8% of the reference value for the ^{137}Cs and ^{60}Co sources, respectively (Spurny and Dachev, 2003). The response of a LIULIN-4 spectrometer (identical in construction to R3DR2 instrument) was compared by Green et al. (2005) to that of the HAWK TEPC (http://www.fwt.com/detector/fw-ad1ds.htm) on 42 aircraft flights in 2003–2004. On all flights, the absorbed dose measured by both instruments agreed to within 5%. We consider that the flux and dose rate errors of the R3DR2 measurements on ISS are within 10%.

The calibrations showed that except for charged energetic particles, the Liulin instruments has a sensitivity towards gamma rays, which allowed monitoring the natural background radiation (Spurny and Dachev, 2002). The detector's neutron sensitivity is minimal for neutrons with energy less than 0.5 MeV and has a maximum of a few percent for neutrons with an energy of 50 MeV (Spurny, 2005). The Hamamatsu PIN diodes of type S2744-08 "neutron induced nuclear counter effect" was described by Zhang et al. (2011). Via this effect neutrons could be observed in all channels of the spectrum.

The semiconductor detector of the R3DR2 instrument was mounted approximately 7 mm below the 0.8 mm thick aluminum cover plate. Furthermore, there was shielding from 0.07 mm copper and 0.2 mm plastic, which provided 0.3 g cm^{-2} of total shielding from the front side. The calculated required kinetic energy of particles arriving perpendicular to the detector was 0.835 MeV for electrons and 19.5 MeV for protons (Berger et al., 2017). This

means that only electrons and protons with energies exceeding the values listed above can cross the R3DR2 shielding materials and reach the detector surface. The detector shielding, being larger from the sides and from behind (Fig. 1), stops all ORB relativistic electrons, attenuates the lower energy IRB protons, but practically does not change the amount of GCR particles.

3 Data analysis and results

The following four primary radiation sources were expected and recognized in the data obtained with the R3DR2 instrument: (i) globally distributed primary GCR particles and their secondary products; (ii) protons in the SAA region of the IRB; (iii) relativistic electrons and/or bremsstrahlung in the high latitudes of the ISS orbit where the ORB is situated; and (iv) solar energetic particles (SEP) in the high latitudes of the ISS orbit. Together with the real SEP particles, a low flux of what were likely to be mostly secondary particles (SP) (protons, neutrons and heavier than H^+ ions) some of them associated with detector interactions were observed in the data. (Neutrons was registered because the "neutron induced nuclear counter effect" described for silicon PIN diodes of Hamamatsu S2744-08 type by Zhang et al. (2011).

In section 3.1 we describe the particle sorting and characterization method. In section 3.2 we verify our results by inspecting the differences in particle deposited-energy spectra. In section 3.3 we discuss the characteristics of the various particle populations observed at the ISS.

3.1 Radiation sources selection procedure

The simplest method for source separation is described by Dachev (2009a) who used the 1971 translation of J. W. Haffner's (Haffner, 1967 and 1971) experimental formulation of the dependence between the incident energy of incoming protons E_p and electrons E_e and the dose to flux ratio (D/F) in nGy cm^2 particle^{-1}:

$$D/F(E_e) = 6x10^{-9}E_e^{-0.9} + 2.5x10^{-8}E_e^{0.15} \quad (2)$$

and

$$D/F(E_p) = 4x10^{-8}E_p^{-0.8} - 6x10^{-10}E_p^{0.85} \quad (3)$$

The valid ranges for formulae (1) and (2) are 1-10 MeV, and 1-1000 MeV, respectively.

Dachev (2009a) shows that according to formulae (2) and (3) the data can be simply split into two parts by using the dose to flux ratio (D/F). When the D/F is less than 1.12 nGy cm^2 particle^{-1}, the expected predominant type of radiation in a 10-s interval is ORB electrons. When the D/F is greater than 1.12 nGy cm^2 particle^{-1}, the expected type of radiation is IRB or SEP protons (Dachev et al. 2012a). The GCR source spans the two ranges. The GCR source was identified by the requirements (Table 1) that their dose rates are less than 15 μGy h^{-1}.

The procedure described by Dachev et al. (2012a) was upgraded. The result of the separation of the four radiation sources (including SP) is seen in Fig. 3, which presents the latitudinal distribution of the dose rates against McIlwain's L values (McIlwain, 1961; Heynderickx et al., 1996). (The ISS orbital data in the paper are calculated by using algorithms by Galperin et al. (1980)). The L value is plotted on the x-axis. On the y-axis, the absorbed dose rate measured by the R3DR2 instrument is plotted. Fig. 3a contains data from

21 June 2015 to 30 June 2015, whereas the Fig. 3b data are from 11 June 2015 to 20 June 2015. Each section contains 86,400 points at a 10-s resolution (10 days x (360 x 24 (hours))).

Four different primary radiation sources separated by the heavy black lines are seen in the data. These sources are plotted in Fig. 3 with different colors for the IRB, ORB, GCR and SEP sources. From one 10-s independent measurement of the dose rate (D) and flux (F), we were able to calculate one dose to flux ratio (D/F). Using this, we were able to decide only what the predominant radiation sources were, but we were unable to extract the exact doses of each source.

The black curve in Fig. 3 was generated by the operator and the interactive separation software. It consists of two parts. The creation of the left part of the black curve starts with the operator setting the point on the vertical abscissa. This point is determined by the upper value of the GCR dose rate of about 10 μGy h^{-1} seen well in Fig. 3 at L-values range 1.00-1.05. Next, the operator moves the cursor to the end point of left part curve where (i) the subtle knee of the GCR source is observed and the GCR dose rate is equal to 15 μGy h^{-1}; (ii) the rising dose rates of the regularly seen IRB and ORB sources are at equal distance from that point or lie on it. The curve of the left part of the black line is asymptote to the GCR values and separates the GCR dose rates from trapped protons in IRB and possible low L-value ORB relativistic electrons. Geomagnetic shielding, measured by the vertical cutoff rigidity (Smart and Shea, 2005), is the reason for reduced GCR fluxes and dose rates at low L-values (Fig. 3) and the slightly rising dose rate toward L-values of 2.5 (Shea et al., 1985). At these increasing L-values the vertical cutoff rigidity decreases and the major amount of the low energy GCR spectra penetrate down to the ISS orbit. At higher L-values, up to L=6, the dose rate has a fixed value because the small increase of the high energy flux of the primary GCR flux don't affect it.

Next, the software draws the right part of the line, which is parallel to the horizontal axis at a dose rate equal to 15 μGy h^{-1}. This is reasonable because the GCR fluxes do not depend strongly on the L-value at high latitudes. Furthermore, the data are distinguished based on two requirements. One is that the ORB data must be above the black line (dose rate >15 μGy h^{-1}) and the second is that the D/F value must be less than 1.12 nGy cm^2 particle^{-1}, whereas the SEP and SP sources are separated above the black line, but the D/F value must be greater than 1.12 nGy cm^2 particle^{-1}. For the ORB source one additional requirement is added -Flux >7 cm^{-2} s^{-1}, which ensures the separation of the ORB from GCR source.

The opportunity to select the left end point of the black line is new compared to the method described by Dachev et al., (2012) where this point was fixed at L=3.5. Also new is allowing the D/F ratio of the points above the left part of the black curve to be below or above 1.12 nGy cm^2 particle^{-1}. This allows identification of ORB relativistic electrons below L=3.5 as shown in Fig. 3a, and as reported recently by Claudepierre et al. (2017) and Turner et al. (2017). Allowing the decision points above the right part of the black curve to be below or above 1.12 nGy cm^2 particle^{-1} is also new, which allows separation of the SEP and SP particles from ORB electrons.

The SP source was found accidentally because it was selected with the same requirements as the SEP source but was seen clearly when SEP events were not observed. Fig. 3b illustrates this in the L range, from 2.5 to 4.

To calculate the daily statistics, the software works with 10 days of un-separated text files with a size of 86,400 lines by 274 columns because each 10-s measurement is characterized by 274 parameters as follows: UT date and time (DD/MM/YYYY; hh:mm:ss);

UT (hh:mm:ss); altitude (km); longitude (deg); latitude (deg); L value; total magnetic field strength B (Gauss); LT (hours); MLT (hours); dip latitude (deg); invariant latitude (deg); flux ($cm^{-2} s^{-1}$); absorbed dose rate ($\mu Gy\ h^{-1}$); D/F(nGy cm^2 particle^{-1}); proton energy (MeV) calculated by the Haffner's formula (Haffner, 1971) only for the points with SD >1.12 nGy cm^2 particle^{-1}; total apparent ambient dose equivalent rate $H*(10)$ ($\mu Sv\ h^{-1}$), calculated as described by Spurny and Dachev (2003); low energy component of $H*(10)_{low}$ ($\mu Sv\ h^{-1}$); high energy component of $H*(10)_{high}$ ($\mu Sv\ h^{-1}$); and 256 values of the count rate in the deposited energy spectrum.

From the primary files, the separation software produces four files with the separated source points and nine daily averaged statistics files for the following parameters: flux, absorbed dose rate, D/F, proton energy, $H*(10),\ H*(10)_{low}\ H*(10)_{high}$, averaged L-value, averaged B and averaged altitude. Furthermore, one more set is produced for the portion of orbits with L>4.

The separation statistics for the 444 days of R3DR2 data give the following results: 3,810,240 points were separated; 2398 were lost (0.062%) or on average less than 6 points per day; and 313 points were counted twice. The average source counts per day were as follows: GCR 7636 points, IRB 573 points, ORB 383 points. The more sporadic SEPs occurred on only 27 days producing 148 points. The average SP counts per 414 days (days without real SEP) were 34 points. In total, the number of daily-averaged measurements for the "stable" sources are the sum of 7636+573+383+34, or 8626 measurements, which were selected from a total of 8640.

All the doses are measured between 24 October 2014 and 11 January 2016 (444 days from the start date to the end date, but not including the end date because the telemetry data don't cover the whole day). GGR source was presented for 444 days of measurements. All other sources are reported for 442 days because of insufficient statistics for 2 days due to telemetry gaps.

The GCR source contributes the majority of the measurements in Fig. 3a/b, which are seen as the area with many red points in the bottom part of the Figs. 3a/b over the L-value range between 1 and 6. The dose rates in the GCR region vary between 0.03 and 15 $\mu Gy\ h^{-1}$.

The second permanent source of radiation corresponds to the protons in the SAA region of the IRB, which are situated as a large maximum in the upper left corner of Fig. 3, with a total of 5876 points in Fig. 3a. They cover L-values between 1.2 and 2.6. The dose rates in the IRB region varied between 10 and 2748 $\mu Gy\ h^{-1}$.

The GCR and IRB sources in both Figures 3a/b look very similar because these two sources have relatively slow time variations. Drastically different are the ORB and SEP sources in the left part of Figures 3a/b. The exact dynamics of the R3DR2 sources between 17 June and 30 June is the topic of a separate paper (Dachev et al., 2016a). Here, we mention only that the magnetic storms on 23 and 25 June and SEP events on 18, 22 and 26 June were the reasons for the drastically different ORB and SEP distributions in Figures 3a/b. The real SEP particles in both figures are seen to appear at some small L-value, then to rise and finally maintain some fixed dose rate value at a range of L from 4 to 6. The SEP source in Fig. 3b appears only at L>5 because the SEP event on 18 May was very weak.

The boundary seen at L=4.7 in the ORB source in Figures 3a/b is generated by the Earth magnetic field hemisphere asymmetries. The ISS orbit in the Southern hemisphere extended up to L=6, while in Northern hemisphere only up to L=4.7.

For most of the EXPOSE-R2 mission observations, the ORB showed a single-maximum L-profile distribution. The double-maxima L-profile distribution in Fig. 3b is part of an extended response to the magnetic storm in March 2015, observed between 20 April and 20 June. After the storms on 23 and 25 June the double-maxima L distributions were seen in the period 15 July-15 August 2015. The "third" Van Allen radiation belt phenomena was recently explained by Mann et al. (2016).

The SP particles are better seen in Fig. 3b, where they cover the L range from 2.4 to 6, whereas the real SEP particles, observed on 18 June 2015, appear at L=5 and rise to a value of 200 µGy h^{-1} at L=6. The upper part of Table 1 contains detailed statistics for the sources presented in Fig. 3a.

3.2 Analysis of the radiation sources from the deposited energy spectra shape

Figure 4 illustrates the different shapes of the deposited energy spectra obtained by the R3DR2 instrument from 21-30 June 2015 (data seen in Fig. 3a) and during the Liulin instrument calibrations with 7.8 MeV proton beam at the cyclotron facility of the University of Louvain, Belgium (Dachev et al., 2002). This figure was created with the aim to confirm the selection procedure described in the previous section and to analyze and validate the SP and SEP spectra shapes, which were first observed in space by the R3DR2 with a DES Liulin-type instrument (Dachev et al., 2015a). Table 1 contains detailed statistics for the spectra presented in Fig. 4. The names of the spectra in Fig. 4 are listed in the first column of the table. The form and shape of the deposited energy spectra also characterize the different radiation sources (Dachev, 2009a).

In Fig. 4, the "PRO" spectrum is a ground-based spectrum obtained at the cyclotron facility at the University of Louvain, Belgium, (Dachev et al., 2002) during the calibrations of Liulin instruments with a 7.8 MeV monoenergetic proton beam falling perpendicularly to the non-shielded detector. The knee seen at about 6.6 MeV corresponds to the point where the incident energy of the normally incident beam on a 0.3 mm thick detector is equal to the deposited energy. All normally incident protons with energies less than 6.3 MeV are stopped in the detector. The exact value of the incident energy at which the CSDA (continuous-slowing-down approximation) range in silicon is 0.3 mm is 6.04 MeV (Berger et al., 2017). Beyond this value, all protons impinging normally are stopped inside the detector. The smaller slope of the "SEP" spectrum beyond the knee can be explained by the presence in space of ions that are heavier than protons and that together with high path protons and neutrons increase the count rate in the high-energy deposition channels of the spectrum.

According to formula (1) the deposited dose rate is the area between the abscissa and the curve of the deposited energy spectrum. The "GCR", "IRB" and "ORB" spectra obtained in the period 21-30 June 2015 are shown in Fig. 4 and Table 1 to validate the R3DR2 data spectra shapes against those described by Dachev (2009a); that is why we will not analyze them further. The L>4 spectrum presents the shape of the GCR spectrum for L>4 values, while the GCR spectrum averages all latitudes of GCR data. The shape of L>4 spectrum is similar to the GCR spectrum. It is above the GCR spectrum because the dose rates are larger at these less geomagnetically-shielded latitudes.

To us, the most interesting and new features are the spectra in Fig. 4 called "SEP", "SEP All" and "SP". In the "Additional table" of Table 1, the statistics of these sources and "PRO" spectrum are described. The "SEP" spectrum includes data only in the maximum of the SEP event on 22 June 2015 (see Table 1), while the "SEP All" spectrum contains data from 21-30 June 2015. As expected, the high-energy deposition part of the SEP spectra is similar to "PRO" spectrum.

The SEP spectra shapes in a range from 0.25-1.0 MeV of deposited energy are similar to the shape of the spectra named "ORB" and "L>4." This is reasonable because GCR, IRB and SEP radiation sources are found in the high latitude regions. The high energy electrons from the ORB source naturally populate the low energy deposition channels of the SEP spectra. The "SEP All" spectrum, collected during the extreme portion of the SEP event, is very similar to the "SEP" spectrum, however in the latter the average dose is smaller since it covers the full range of the event. (see Table 1).

As mentioned above the SP source was found accidentally because it provides SEP-like doses when SEP events were not observed. Fig. 3b illustrates this in the L range, from 2.5 to 4. The magenta points in this range were not produced by SEP protons because the SEP event on 18 June 2015 was too weak to produce real points at such low latitudes. Real SEP points are seen at a range above L=5.

To collect enough points for the SP spectrum, we extended the time period from 21 March to 10 June 2015 (see Table 1). The following conclusions can be made about the SP spectrum: (i) in the range from 0.25-2.0 MeV deposited energy it is similar to the shape of the "ORB" and "L>4" spectra for the same reasons as described for the SEP spectrum; (ii) in the range from 2-10 MeV, the deposited energy is elevated in comparison with the "L>4" spectra. This can be explained with the additional high energy deposition source as energetic protons; (iii) in the range above 10 MeV, the shape is completely different than any other spectrum in Fig. 4 and can be explained only with sporadic hits of the detector by secondary long-path low energy protons, neutrons and heavier than H^+ ions generated within the detector or in materials very nearby.

Section 3.1 of the article explains in detail how the data selection was performed. The different forms of spectra seen in section 3.2 validate the selection methodology. The selection method described in Section 3.1 (Dachev, 2009) was based on the dependence of the dose rate from the particles flux. This method in this section was applied in (Dachev at al., 2016a) for the 21-30 June 2015 time period and also validates the selection validity.

3.3 Radiation source analysis

3.3.1 GCR radiation source

Fig. 5 presents the variations of the GCR daily averaged flux and dose rates during the period from 24 October 2014-11 January 2016 together with variations in the F10.7 radio flux index data (http://www.swpc.noaa.gov/products-and-data) in the top panel of Fig. 5 and Oulu neutron monitor (NM) data (https://cosmicrays.oulu.fi/) in the bottom panel of Fig. 5.

The major finding is that the F10.7 radio flux index seen in the top panel did have a descending linear trend because the measurements were performed in the declining phase of the 24th solar cycle. The effect of solar modulation (Potgieter, 2013) assumes a rising trends in the Oulu NM GCR count rate and in the R3DR2 GCR dose rate and flux measurements, respectively (please see the black dashed lines in both panels). The daily average dose rate data trend had a minimum value of 71 µGy d⁻¹ at the beginning of the measurements in October of 2014 and maximum of 72 µGy d⁻¹ at the end of observations in January of 2016.

We compared the averaged R3DR2 GCR daily dose rate data of approximately 71.6 µGy d⁻¹ with those measured inside the ISS by the DOSTEL 1 and DOSTEL 2 instruments (Burmeister et al., 2015) for the period from 24 October 2014 – 29 July 2015: Both DOSTEL instruments showed averaged daily values in the range of 140-150 µGy d⁻¹ which were larger than those obtained by R3DR2. We accept this result as confirmation of the theoretical

calculations performed by Mrigakshi et al., (2013) (see Fig. 4b therein) showing that the absorbed dose rates in a water sphere with a smaller Aluminum shield thickness are smaller than the doses obtained behind a larger shield thickness. The R3DR2 data were obtained outside of the ISS, behind 0.3 g cm^{-2} shielding, whereas the DOSTEL 1 and DOSTEL 2 instrument data were measured behind more shielding, inside of the ISS.

Mrigakshi et al. (2013) calculated the dose rate at ISS altitudes for 0.3 g cm^{-2} of aluminum shielding in 2014 as approximately 68 μGy d^{-1}, which is closer to the value of 71.6 μGy d^{-1} measured by the R3DR2 instrument during the period from 24 October - 31December 2014. According to the Mrigakshi et al., (2013) (see Fig. 4b therein) calculations of the DOSTEL 1 and DOSTEL 2 instruments averaged absorbed dose rates of approximately 140 μGy d^{-1} seem to be obtained behind larger than 40 g cm^{-2} shielding.

The averaged R3DR2 GCR daily dose rate and flux also exhibited short-term variations, which generally correlate with the Oulu NM minute count rate and reflect the periods with Forbush decreases (Forbush, 1954) that are connected with the magnetic storm and substorm periods in the GCR data. Most remarkable are the decreases that coincide with the two largest in the data magnetic storms on 16 March and 22 June 2015.

The R3DR2 GCR daily dose rate averaged over 444 days was calculated to be 71.6 μGy d^{-1} with a minimum value of 59 μGy d^{-1} and maximum value of 77 μGy d^{-1}. The total accumulated dose for 444 days is 31.8 mGy.

3.3.2 IRB radiation source

The IRB source is the second source, apart from GCR, that was observed every day in the R3DR2 data. The profile of the IRB source dependent on the L value is clearly seen in the left part of Fig. 3a and 3b.

Fig. 6 plots the daily average fluxes (in cm^{-2} s^{-1}) (green), dose rates (blue) and the maximal hourly dose rate (red), measured by the R3DR2 instrument on the ISS from 24 October 2014 to 11 January 2016. These values are plotted according to the left vertical axes. Along the right axes the average altitude of the station is plotted, which was obtained together with the average daily values of the flux and dose rate.

The flux and dose rate were large during the interval from October-December of 2014; then, they fell until the end of June 2015 and increased again until the end of the measurements. These long-term variations correlated well with the variations in the average altitude of the station. The altitudinal dependence in the bottom part of the IRB was investigated by the R3DR data (Dachev et al., 2015b). This is a well-known phenomenon that has been competently described elsewhere (Filz & Holeman, 1965; Gusev et al., 2003). Therefore, it will not be discussed further here.

Higher fluxes and doses at the end of the mission, and a linear rising trend in the flux values, are connected with lower solar activity and a lower sink of the IRB protons, respectively, in the decreased neutral atmosphere density (Qian and Solomon, 2012).

Obvious depletions in the IRB flux, the daily and hourly maximal doses were observed in the recovery phase of the magnetic storms presented with the Dst curve at the top of Fig. 7. We assume that the effect is similar to the described by Zou et al., (2011).

The descending-orbits hourly IRB flux and dose rate values are smaller by a factor of 0.7 in comparison with the ascending ones (Dachev et al., 2016a), which can be explained by the east-west asymmetries of the proton fluxes in the region of the SAA (Wilson et al., 2007; Chernykh et al., 2008). The simplified explanation is that the R3DR2 detector, which was

located on the left side of the ISS "Zvezda" module opposite the ISS vector of velocity, was shielded more by the "Zvezda" module body on the descending orbits from west to east drifting inner belt protons, when the ISS was in the nominal "XVV" orientation (http://spaceflight.nasa.gov/station/flash/iss_attitude.html).

The R3DR2 IRB daily dose rate averaged over 442 days was calculated to be 567 μGy d^{-1} with a minimal value of 340 μGy d^{-1} and maximal value of 844 μGy d^{-1}. The total accumulated dose for 442 days is 251 mGy.

3.3.3 ORB radiation source

Fig. 7 presents the ORB radiation source variations during the period from 24 October 2014 - 11 January 2016. The upper panel of Fig. 7 presents the Dst index variations (http://wdc.kugi.kyoto-u.ac.jp/index.html) (red line), which were obtained online from the World Data Center for Geomagnetism, in Kyoto, Japan.

The lower panel presents the variations of 2 parameters. The first one is the daily average relativistic electron dose rate as measured in ORB with the R3DR2 instrument on the ISS (black heavy line). Two periods are clearly seen in the data. In the relatively "quiet" period between 24 October 2014 and the middle of March 2015, the ORB daily dose rate was relatively small and varied during the interval by 2-200 μGy h^{-1}. During the second period, between the middle of March 2015 and the end of the observations, strong variations in the ORB daily dose rate were observed. The largest maxima (up to 3000 μGy h^{-1}) in the ORB source anti-correlate well with the Dst index variations in the upper panel of Fig. 7 (red line).

The daily dynamics of the ORB flux and dose rate from 17-30 June was presented by Dachev et al. (2016a) (see Fig. 4 therein), where the well-known features of the ORB fluxes close to the magnetic storm are clearly seen, as follows: strong depletion of the ORB flux during the main phase of the magnetic storm on 22 June 2015, with an increase of the flux after the storm and next, a depletion and increase after and during the storm on 25 June. Very similar relativistic electron dynamics in dose rate and L position in dependence on the geomagnetic activity were studied by the R3DR instruments on the ISS (Dachev et al., 2012b).

The second parameter (MetOp Index or MO2 Index) presented by a heavy green line in Fig. 7b is the "Index of relative intensities of >300 keV electrons (90 deg. detector) in the outer belt (L value>2.5), from the NOAA SEM-2 instrument" (https://www.ngdc.noaa.gov/stp/satellite/poes/) with the data from MetOp-2 satellite launched under the Meteorological Operational Satellite Program in Europe (https://directory.eoportal.org/web/eoportal/satellite-missions/m/metop). According to the NOAA scientists: "The belt indices are a measure of the integrated difference, or departure, of individual sensor responses observed on a given day from the responses of those sensors as averaged over the previous year's observations" (http://legacy-www.swpc.noaa.gov/ftpdir/lists/bi/old_bi/README).

The comparison of the R3DR2 daily dose curve with the MO2 index curve shows relatively good correlation, although both satellites were in different orbits. The ISS orbit was at approximately 415 km altitude from the Earth's surface and at 51.6° orbit inclination, whereas the MetOp (MO2) satellite was at a mean altitude of 817 km with an inclination of 98.7°. The similarity of the curves verifies the R3DR2 separation procedure, considering that MO2 index, derived from much higher time resolution data from the more sophisticated, heavier and power-consuming SEM-2 instrument was expected to be more reliable than those from the single detector R3DR2 instrument.

The R3DR2 ORB daily dose rate averaged over 442 days was calculated to be 278 µGy d^{-1} with a minimal value of 2 µGy d^{-1} and maximal value of 2,962 µGy d^{-1}. The total accumulated dose for 442 days is 123 mGy.

3.3.4 SEP radiation source

Fig. 8 presents the averaged SEP daily dose rate variations, measured with R3DR2 on the ISS for the period from 24 October 2014-11 January 2016. These are plotted together with the solar proton fluxes measured in the geosynchronous orbit with the GOES 15 Space Environment Monitor (SEM) instrument (http://goes.gsfc.nasa.gov/text/databook/section05.pdf), with energies more than 10 (red curve) to 100 MeV (blue curve) plotted. We call the low dose rates of a few µGy d^{-1} seen along the bottom of Fig. 8 secondary particle (SP) sources. These were generated by GCR particles inside the instrument and surrounding EXPOSE-R2 material and consists mainly of protons and neutrons.

Eleven maxima are seen in the R3DR2 SEP daily dose rate variations in the bottom of Fig. 8. All of them coincide well with the >10 MeV GOES SEM maxima. The >100 MeV proton flux channel on GOES had only one well-seen maximum on 29 October 2015, which is also measured with the R3DR2 instrument. The largest maximum, up to almost 3000 µGy d^{-1} on 22 June 2015, was not observed in the GOES >100 MeV channel; however, if a virtual extravehicular activity (EVA) was performed during the period of this SEP maximum, the obtained doses on the skin of cosmonauts/astronauts could have reached 2.84 mGy over six and a half hours, which is identical to the average absorbed dose obtained inside of the ISS over 15 days (Reitz at al., 2005, Dachev et al., 2016a).

The R3DR2 SEP+SP daily dose rate averaged over 442 days was calculated to be 9 µGy d^{-1} with a minimum value of 0.64 µGy d^{-1} and maximum value of 2,848 µGy d^{-1}. The total accumulated dose for 442 days is 4 mGy.

As we already mentioned the shape of the SP spectrum in Fig. 4 above 2 MeV is completely different than any other spectra there and can be explained only with sporadic hits of the detector by long-path low-energy protons, neutrons and heavier than H^{+} ions. All SP radiation was obtained in high latitudes of both hemispheres (see Table 1, which is why we conclude that the observed SP were generated by GCR primary source (Dyer et al., 1985). The expected larger SP flux in the IRB region of the SAA can't be identified because they are selected with the same requirements as the IRB protons.

The secondary protons, neutrons and heavier than H^{+} ions contribution was calculated excluding the part of spectra up to 2 MeV, which is predominantly produced by primary GCR and ORB particles. We found that the average integral flux of the SP in R3DR2 detector was 0.16 cm^{-2} s^{-1}, which is about 3 times smaller than the calculated by Armstrong and Colborn (2001) flux of GCR secondary protons for the ISS compartments. The difference can be explained with larger secondary flux in the heavier shielded ISS compartments than the R3DR2 small shielding of 0.3 g cm^{-2}.

The average contaminated with GCR and ORB particles hourly dose rate from SP was 17.1 µGy h^{-1}, while the dose rate from the SP spectrum above 2 MeV was 9.7 µGy h^{-1}. The average contaminated daily SP dose rate was 1.9 µGy d^{-1}, while the pure SP daily dose rate was 1.1 µGy d^{-1}.

3.3.5 Summary from all sources

The total average daily dose rate is calculated by the sum of all sources: 71.6 (GCR for 444 days) +567 (IRB for 442 days) +278 (ORB for 442 days) +9 (SEP+SP for 442 days)=925.6 μGy d^{-1}. The total accumulated dose for the period 24 October 2014-11 January 2016 is 409.8 mGy.

If we wish to calculate an average equivalent daily dose rate we have to summarize the following: 3.5*71.6 (GCR)+1.3*567 (IRB)+1*278 (ORB)+1.3*9 = 1,277.4 μSv d^{-1}. We assume following biological effectiveness (Q): GCR=3.5, IRB=1.3, ORB=1 and SPE+SP=1.3). The 30 days value is: 0.0383 mSv, while for 1 year (365 days) is 0.4658 Sv. (All dose rate statistics of the measured by R3DR2 instrument data are presented in Table 2.)

4 Conclusions

The R3DR2 instrument data measured in the ESA EXPOSE-R2 platform outside of the Russian "Zvezda" module of the ISS during the period from 24 October 2014- 11 January 2016, at an average altitude of 415 km and 51.6° orbit inclination are presented and analyzed in this paper.

The new radiation source selection procedure described in this paper is based on a specially developed novel procedure, with experimentally obtained formulas for describing the relationships between the dose to flux ratio (Haffner, 1967; 1971) and type of predominant radiation.

For the first time in the R3DR2 DES data, the following four radiation sources of the ISS environment were simultaneously selected and analyzed: (i) galactic cosmic ray (GCR) particles and their secondary products, with an average daily dose rate of 71.6 μGy d^{-1}; (ii) protons in the South Atlantic Anomaly (SAA) region of the inner radiation belt (IRB), with an average daily dose rate of 567 μGy d^{-1}; (iii) relativistic electrons and/or bremsstrahlung in the outer radiation belt (ORB), with an average daily dose of 278 μGy d^{-1}, and a range from near zero in magnetically quiet days to almost 3000 μGy d^{-1} during periods after magnetic storms; and (iv) 12 solar energetic particle (SEP) events were observed in the data. During the largest SEP event on 22 June 2015, the hourly dose rate reached more than 5000 μGy h^{-1} (Dachev et al., 2016a).

The EXPOSE-R2 mission (2014-2016) GCR daily averaged dose rate of 71.6 μGy d^{-1} is lower than the EXPOSE-E 2008-2009 mission value of 91.1 μGy d^{-1} (Dachev et al., 2012a,) and EXPOSE-R 2009-2010 mission value of 81.4 μGy d^{-1} (Dachev et al., 2015b) because the solar modulation (Potgieter, 2013) lowered the GCR doses during 2014-2016.

The daily averaged IRB doses from the 3 instruments R3D/E/R/R2 increased as follows: 426, 506, and 567 μGy d^{-1}, with the main reason for this increase being a rise in average altitude of the ISS since 2008.

The EXPOSE-R2 mission (2014-2016) ORB daily-averaged dose rates were high compared with the other two EXPOSE missions onboard the ISS because the 2014-2016 mission occurred with the highest solar and geomagnetic activity, which stimulated the particle acceleration processes in the magnetosphere.

R3DR2 source doses were compared with the DOSimetric TELescope instrument DOSTEL doses from April 13th to June 30th 2004 during the MTR-1 mission phase outside ISS (Labrenz et al., 2015). DOSTEL values were: 77.6 μGy d^{-1} for GCR source and 296.1 μGy d^{-1} for IRB source. It is seen that DOSTEL and R3DR2 GCR doses are very similar

(71.6 and 77.6 μGy d^{-1}), while the larger R3DR2 IRB dose of 576 μGy d^{-1} has a simple explanation associated with higher altitude of ISS during the R3DR2 mission.

The additional dose rate measured with DOSTEL instrument outside ISS due to the enhanced particle flux (EPF) (This is the term, which they use for the ORB electron flux), from September 24th to October 8th 2004 was calculated to be ~130 Gy d^{-1}. The twice larger (278 μGy d^{-1}) daily average ORB dose rate, measured with the R3DR2 instrument for the period 24 October 2014 - 11 January 2016, is explained as a result of larger geomagnetic activity.

To answer the question about how harmful the obtained dose rates were, during the relatively low solar maximum and decline of 2014-2016, we compare the average equivalent dose for 30 days calculated from the R3DR2 instrument data of ~0.0383 Sv with the NCRP (Report 132) recommendations for the dose limits in low earth orbit of 1.0 Sv for eyes and 1.5 Sv for skin and found that the R3DR2 doses are much smaller than the maximum recommended safety level. The eye and skin shielding inside the US and Russian space suits are nearly the same as the R3DR2 shielding of 0.3 g cm^2 (Benton et al., 2006). The same is true for 1 year of eye and skin limits, which are 1.5 and 3 Sv, respectively, whereas the calculated R3DR2 dose is 0.466 Sv. (All dose rate calculations are presented in Table 2.)

References

Armstrong T.W., B.L. Colborn, (2001) Predictions of secondary neutrons and their importance to radiation inside the international space station, Radiation Measurements, 33, 229–234.

Badavi, F.F., (2014), Validation of the New Trapped Environment AE9/AP9/SPM at Low Earth Orbit, Advances in Space Research, 54, 917-928, http://dx.doi.org/10.1016/j.asr.2014.05.010.

Benton, E.R., Benton, E.V., (2001), Space radiation dosimetry in low-Earth orbit and beyond, Nucl. Instrum. and Methods in Physics Research, B, 184, (1-2), 255-294.

Benton, E.R., Benton, E.V., Frank, A.L., Moyers, M.F., (2006), Characterization of the radiation shielding properties of US and Russian EVA suits using passive detectors. Radiat. Meas. 41, 1191–1201.

Berger, M.J., J.S. Coursey, M.A. Zucker, J. Chang, (2017), Stopping-Power and Range Tables for Electrons, Protons, and Helium Ions, NIST Standard Reference Database 124. Available online at: http://physics.nist.gov/PhysRefData/Star/Text/contents.html.

Beaujean R., J. Kopp, S. Burmeister, F. Petersen, G. Reitz, (2002) Dosimetry inside MIR station using a silicon detector telescope (DOSTEL), Radiation Measurements, 35, 433 – 438.

Burmeister, S., T. Berger, J. Labrenz, B. Boehme, L. Haumann, G. Reitz, 2015. The DOSIS and DOSIS 3D experiments on-board the International Space Station – Current Status and Latest Data from the DOSTELs as Active Instruments, Workshop on Radiation Measurements on ISS, Cologne, Germany, September 8–10, 2015, Available online at: http://wrmiss.org/workshops/twentieth/Burmeister.pdf.

Cucinotta, F.A., M.R. Shavers, P.B. Saganti, J. Miller, Editors, Radiation Protection Studies of International Space Station Extravehicular Activity Space Suits, NASA/TP-2003-212051, pp 2, December 2003, Available online at: https://ntrs.nasa.gov/archive/nasa/casi.ntrs.nasa.gov/20040031719.pdf.

Chernykh, I., V. Petrov, V. Shurshakov, et al., (2008), ISS attitude influence on the dose rate measured with Liulin-5 instrument, Workshop on Radiation Measurements on ISS, Krakow, Poland, 8-10 September, Available online at: http://wrmiss.org/workshops/thirteenth/Chernykh.pdf.

Claudepierre, S. G., T. P. O'Brien, J. F. Fennell, J. B. Blake, J. H. Clemmons, M. D. Looper, J. E. Mazur, J. L. Roeder, D. L. Turner, G. D. Reeves, H. E. Spence, (2017), The hidden dynamics of relativistic electrons (0.7-1.5 MeV) in the inner zone and slot region, J. Geophys. Res. Space Physics, 122, http://dx.doi.org/10.1002/2016JA023719.

Dachev, Ts., B. Tomov, Yu. Matviichuk, Pl. Dimitrov, J. Lemaire, G. Gregoire, M. Cyamukungu, H. Schmitz, K. Fujitaka, Y. Uchihori, H. Kitamura, G. Reitz, R. Beaujean, V. Petrov, V. Shurshakov, V. Benghin, F. Spurny, (2002) Calibration Results Obtained With Liulin-4 Type Dosimeters, Adv. Space Res., V 30, No 4, 917-925, http://dx.doi.org/10.1016/S0273-1177(02)00411-8.

Dachev, Ts.P., (2009a), Characterization of near Earth radiation environment by Liulin type instruments, Adv. Space Res., 44, 1441-1449, http://dx.doi.org/10.1016/j.asr.2009.08.007.

Dachev, Ts.P., B.T. Tomov, Yu.N. Matviichuk, P.G. Dimitrov, N.G. Bankov, (2009b), Relativistic Electrons High Doses at International Space Station and Foton M2/M3 Satellites, Adv. Space Res., 44, 1433-1440, http://dx.doi.org/10.1016/j.asr.2009.09.023.

Dachev, Ts.P., J. Semkova, B. Tomov, Yu. Matviichuk, Pl. Dimitrov, R. Koleva, St. Malchev, G. Reitz, G. Horneck, G. De Angelis, D.-P. Häder, V. Petrov, V. Shurshakov, V. Benghin, I. Chernykh, S. Drobyshev, N. G. Bankov, (2011), Space Shuttle drops down the SAA doses on ISS, Adv. Space Res., 47, 2030-2038, http://dx.doi.org/10.1016/j.asr.2011.01.034.

Dachev, Ts., G. Horneck, D.-P. Häder, M. Lebert, P. Richter, M. Schuster, R. Demets, (2012a), Time profile of cosmic radiation exposure during the EXPOSE-E mission: the R3D instrument. Internat. Journal of Astrobiology, 12, 5, 403-411, http://eea.spaceflight.esa.int/attachments/spacestations/ID501800a9c26c2.pdf.

Dachev, Ts.P., B.T. Tomov, Yu.N. Matviichuk, Pl.G. Dimitrov, N.G. Bankov, G. Reitz, G. Horneck, D.-P. Häder, M. Lebert, M. Schuster, (2012b), Relativistic Electron Fluxes and Dose Rate Variations during April-May 2010 Geomagnetic Disturbances in the R3DR Data on ISS, Adv. Space Res., 50, 282–292, http://dx.doi.org/10.1016/j.asr.2012.03.028.

Dachev Ts., (2013), Analysis of the space radiation doses obtained simultaneously at 2 different locations outside ISS, Adv. Space Res., 52, 1902-1910, http://dx.doi.org/10.1016/j.asr.2013.08.011.

Dachev, T.P., J.V. Semkova, B.T. Tomov, Yu.N. Matviichuk, P.G. Dimitrov, R.T. Koleva, St. Malchev, N.G. Bankov, V.A. Shurshakov, V.V. Benghin, E.N. Yarmanova, O.A. Ivanova, D.-P., Häder, M. Lebert, M.T. Schuster, G. Reitz, G. Horneck, Y. Uchihori, H. Kitamura, O. Ploc, J. Kubancak, I. Nikolaev, (2015a), Overview of the Liulin type instruments for space radiation measurement and their scientific results, Life Sciences in Space Research, 4, 92-114, http://dx.doi.org/10.1016/j.lssr.2015.01.005.

Dachev, Ts., G. Horneck, D.-P. Häder, M. Schuster, and M. Lebert, (2015b), EXPOSE-R cosmic radiation time profile, Internat. Journal of Astrobiology, 14, 17-25, http://dx.doi.org/10.1017/S1473550414000093 and http://journals.cambridge.org/article_S1473550414000093.

Dachev, T.P., B.T. Tomov, Yu.N. Matviichuk, Pl. G. Dimitrov, N.G. Bankov, (2016a) High dose rates obtained outside ISS in June 2015 during SEP event, Life Sciences in Space Research, Life Sciences in Space Research, 9, 84-92, 2016, http://dx.doi.org/10.1016/j.lssr.2016.03.004.

Dachev T.P., N. G. Bankov, G. Horneck, D.-P. Häder, (2016b), EXPOSE-R2 cosmic radiation time profile (Preliminary results), Letter to the Editor, Radiat Prot. Dosimetry 2016 1-4, https://doi.org/10.1093/rpd/ncw123.

Damasso, M., Ts. Dachev, G. Falzetta, M.T. Giardi, G. Rea, A. Zanini, (2009), The radiation environment observed by Liulin-Photo and R3D-B3 spectrum-dosimeters inside and outside Foton-M3 spacecraft, Radiation Measurements, 44, N0 3, 263-272, doi:10.1016/j.radmeas.2009.03.007.

Dyer, C.S., P.R. Truscott, H. Evans, A. J. Sims, N. Hammond and C. Comber, (1996) Secondary radiation environments in heavy space vehicles and instruments, Adv. Space Res., 17, 53-58.

De Vera J.-P., U. Boettger, R. de la Torre Noetzel, F.J. Sánchez, D. Grunow, N. Schmitz, C. Lange, H.-W. Hübers, D. Billi, M. Baqueé, P. Rettberg, E. Rabbow, G. Reitz, T. Berger, R. Möller, M. Bohmeier, G. Horneck, F. Westall, J. Jänchen, J. Fritz, C. Meyer, S. Onofri, L. Selbmann, L. Zucconi, N. Kozyrovska, T. Leya, B. Foing, R. Demets, C.S. Cockell, C. Bryce, D. Wagner, P. Serrano, H.G.M. Edwards, J. Joshi, B. Huwer, P. Ehrenfreund, A. Elsaesser, S. Ott, J. Meessen, N. Feyh, U. Szewzyk, R. Jaumann, T. Spohn, (2012), Supporting Mars exploration: BIOMEX in Low Earth Orbit and further astrobiological studies on the Moon using Raman and PanCam technology. Planet. Space Sci. 74, 103–110.

Di Fino, L, V. Zaconte, M. Stangalini, R. Sparvoli, P. Picozza, et al., (2014), Solar particle event detected by ALTEA on board the International Space Station, J. Space Weather Space Clim., 4, A19, http://dx.doi.org/10.1051/swsc/2014015.

Filz, R. & E. Holeman, (1965), Time and altitude dependence of 55-MeV trapped protons, August 1961 to June 1964. J. Geophys. Res. 70(23), 5807-5822.

Forbush, S.E., (1954), World-wide cosmic ray variations, 1937–1952. Journal of Geophysical Research, 59(4), 525-542.

Galperin, Yu.I., Ponamarev, Yu.N., and Sinizin, V.M. (1980), Some algorithms for calculation of geophysical information along the orbit of near Earth satellites. Report No 544, Space Research Institute, Moscow. (In Russian).

Gusev, A.A., G.I., Pugacheva, U.B. Jayanthi, & N. Schuch, (2003), Modeling of low-altitude Quasi-trapped proton fluxes at the equatorial inner magnetosphere. Braz. J. Phys. 33, 775–781.

Heynderickx, D., J. Lemaire, E.J. Daly, (1996), Historical review of the different procedures used to compute the L-parameter, Radiat. Meas., 26, 325-331.

Haffner, J.W. (1967), Radiation and shielding in space, Academic Press, NY (1967).

Haffner, J.W., Yadernoe izluchenie i zashchita v kosmose (Nuclear Radiation and Protection in Space), pp 115, Atomizdat, Moscow, 1971. (book in Russian), translated from: J. W. Haffner, Radiation and shielding in space, Academic Press, NY (1967).

Häder, D.-P., and T.P. Dachev, (2003), Measurement of solar and cosmic radiation during spaceflight, Kluwer Press, Surveys in Geophysics, 24, 229-246.

Häder, D.P., P. Richter, M. Schuster, M., Ts. Dachev, B. Tomov, Pl. Dimitrov, Yu. Matviichuk, (2009), R3D-B2 - Measurement of ionizing and solar radiation in open space in the BIOPAN 5 facility outside the FOTON M2 satellite, Adv. Space Res., 43, 8, 1200-1211, http://dx.doi.org/12.0301016/j.asr.2009.01.021.

Horneck, G., (1994), HZE particle effects in space, Acta Astronautica, 32, 749–755.

Labrenz, J, Burmeister S, Berger T, Heber B & Reitz G., (2015), Matroshka DOSTEL measurements onboard the International Space Station (ISS). J. Space Weather Space Clim., 5, A38, 2015, DOI: 10.1051/swsc/2015039.

Larosa, M., F. Agostini, M. Casolino, C. Santis, L. De, Fino, C. La Di Tessa, L. Narici, P. Picozza, A. Rinaldi, and V. Zaconte, (2011), Ion rates in the International Space Station during the December 2006 Solar Particle Event, Journal of Physics G: Nuclear and Particle Physics, 38, 9, 95-102, http://dx.doi.org/10.1088/0954-3899/38/9/095102.

Mann, I.R., L.G. Ozeke, K.R. Murphy, S.G. Claudepierre, D.L. Turner, D.N. Baker, I.J. Rae, A. Kale, D.K. Milling, A.J. Boyd, and H.E. Spence, (2016), Explaining the dynamics

of the ultra-relativistic third Van Allen radiation belt, Nature Physics, 12(10), 978-983.

McIlwain, C.E., (1961), Coordinates for mapping the distribution of magnetically trapped particles. J. Geophys. Res. 66, 3681–3691.

Mrigakshi, A.I., D. Matthiä, T. Berger, G. Reitz, R.F. Wimmer-Schweingruber, (2013), Estimation of galactic cosmic ray exposure inside and outside the Earth's magnetosphere during the recent solar minimum between solar cycles 23 and 24, Advances in Space Research, 52, 979-987, http://dx.doi.org/doi:10.1016/j.asr.2013.05.007.

Narici, L., M. Casolino, L. Di Fino, M. Larosa, P. Picozza, V. Zaconte, (2015), Radiation survey in the International Space Station, Journal of Space Weather and Space Climate, 5:A37.

National Council on Radiation Protection and Measurements, 2000, Recommendations of Dose Limits for Low Earth Orbit, NCRP Report 132, Bethesda MD, 2000.

Nealy, J.E., F.A. Cucinotta, J.W. Wilson, F.F. Badavi, N. Zapp, T. Dachev, B.T. Tomov, E. Semones, S.A. Walker, G.De Angelis, S.R. Blatting, W., Atwell, (2007), Pre-engineering spaceflight validation of environmental models and the 2005 HZETRN simulation code. Adv. Space Res., 40, 11, 1593-1610, http://dx.doi.org/10.1016/j.asr.2006.12.030.

Petrov, M.V., V.S. Machmutov, N.A. Panova, V.V. Shurshakov, T.P. Dachev, Y.N. Matviichuk, J.V. Semkova, (1994), Peculiarities of the Solar Proton Events of October 19, 1989 and March 23, 1991 According to the Measurements on board the MIR Space Station, Adv. Space Res., 14, 645-650, http://dx.doi.org/10.1016/0273-1177(94)90520-7.

Potgieter, M.S., Solar Modulation of Cosmic Rays, (2013), Living Rev. Solar Phys., 10, (2013), 3, http://www.livingreviews.org/lrsp-2013-3.

Qian, L. and S. C. Solomon, (2012), Thermospheric density: an overview of temporal and spatial variations, Space Sci Rev 168:147–173, http://download.hao.ucar.edu/pub/stans/papers/QianSSR2012.pdf.

Rabbow, E., P. Rettberg, S. Barczyk, M. Bohmeier, A. Parpart, C. Panitz, G. Horneck, R. von Heise-Rotenburg, T. Hoppenbrouwers, R. Willnecker, P. Baglioni, R. Demets, J. Dettmann, G. Reitz, (2012), EXPOSE-E: An ESA astrobiology mission 1.5 years in space. Astrobiology, 12, 374-386

Rabbow, E., et al., (2015), The astrobiological mission EXPOSE-R on board of the International Space Station, International Journal of Astrobiology, 14, 3-16, http://dx.doi.org/10.1017/S1473550414000202.

Reitz, G., R. Beaujean, E. Benton, S. Burmeister, Ts. Dachev, S. Deme, M. Luszik-Bhadra, P. Olko, (2005), Space radiation measurements on-board ISS-the DOSMAP experiment, Radiat Prot Dosimetry, 116, 374-379, http://rpd.oxfordjournals.org/cgi/content/abstract/116/1-4/374.

Semkova, J., T. Dachev, R. Koleva, N. Bankov, S. Maltchev, V. Benghin, V. Shurshakov, V. Petrov, (2014), Observation of radiation environment in the International Space Station in 2012–March 2013 by Liulin-5 particle telescope. J. Space Weather Space Clim., 4, A32, http://dx.doi.org/10.1051/swsc/2014029.

Schuster, M., T. Dachev, P. Richter, D.P. Häder, (2012), R3DE: Radiation Risk Radiometer-Dosimeter on the International Space Station—optical radiation data recorded during 18 months of EXPOSE-E exposure to open space. Astrobiology. May 12, 393-402, http://dx.doi.org/10.1089/ast.2011.0743.

Shurshakov, V. A., Petrov, V. M., Ivanov, Yu.V, Bondarenko, V.A., Tzetlin, V.V., Makhmutov, V.S., Dachev. Ts.P. and Semkova, J. V. Solar particle events observed on MIR station, Radiation Measurements, Volume 30, Issue 3, 317-325, 1999, http://dx.doi.org/10.1016/S1350-4487(99)00058-X.

Smart, D.F., M.A. Shea, (2005), A review of geomagnetic cutoff rigidities for earth-orbiting spacecraft, Adv. Space Res., 36, 2012–2020.

Shea, M.A., D.F., Smart, L.C. Gentile, The use of the McIlwain L-parameter to estimate cosmic ray vertical cutoff rigidities for different epochs of the geomagnetic field, (1985), In NASA. Goddard Space Flight Center 19th Intern. Cosmic Ray Conf., Vol. 5 p 332-335, http://articles.adsabs.harvard.edu//full/1985icrc....5..332s/E000332.000.htmlSimpson, J.A., (1983), Composition and origin of cosmic rays. In: Shapiro, M.M. (Ed.), NATO ASI Series, Series C Mathematical and Physical Sciences, 107. Reidel, Dordrecht.

Slaba, T.C., S.R. Blattnig, F.F. Badavi, N.N. Stoffle, R.D. Rutledge, K.T. Lee, E.N. Zapp, T.P. Dachev, B.T. Tomov, (2011), Statistical Validation of HZETRN as a Function of Vertical Cutoff Rigidity using ISS Measurements. Adv. Space Res., 47, 600-610, doi:10.1016/j.asr.2010.10.021.

Slaba, T.C., A.A. Bahadori, B.D. Reddell, R.C. Singleterry,; M.S. Clowdsley, S.R. Blattnig, (2017), Optimal shielding thickness for galactic cosmic ray environments, Life Sciences in Space Research, 12, 1-15, http://dx.doi.org/10.1016/j.lssr.2016.12.003.

Smart, D. F., M. A. Shea, T. P., Dachev, N. G. Bankov, V. M. Petrov, V. V. Benghin, (1994), The Dose Rate Observed on 19-21 October 1989 and its Modulation by Geophysical Effects, Adv. Space Res., 14, 651-654, http://dx.doi.org/10.1016/0273-1177(94)90521-5.

Spurny, F., Ts. Dachev, (2003), Long-term monitoring of the onboard aircraft exposure level with a Si-diode based spectrometer. Adv. Space Res.32 (1), 53–58, http://dx.doi.org/10.1016/S0273-1177(03)90370-X.

Turner, D. L., T. P. O'Brien, J. F. Fennell, S. G. Claudepierre, J. B. Blake, A. N. Jaynes, D. N. Baker, S. Kanekal, M. Gkioulidou, M. G. Henderson and G. D. Reeves, (2017), Investigating the source of near-relativistic and relativistic electrons in Earth's inner radiation belt, J. Geophys. Res. Space Physics, 122, 695–710, doi:10.1002/2016JA023600.

Uchihori, Y., H. Kitamura, K. Fujitaka, Ts.P. Dachev, B.T. Tomov, P.G. Dimitrov, Y. Matviichuk, Analysis of the calibration results obtained with Liulin-4J spectrometer-dosimeter on protons and heavy ions, Radiation Measurements, 35, 127-134, 2002, http://dx.doi.org/10.1016/S1350-4487(01)00286-4 .

Wilson J.W., J. E. Nealy, T.P. Dachev, B.T. Tomov, F. A. Cucinotta, F. F. Badavi, G.De Angelis, N. Leutke, W. Atwell, (2007), Time serial analysis of the induced LEO environment within the ISS 6A, Adv. Space Res., 40, 11, 1562-1570, http://dx.doi.org/10.1016/j.asr.2006.12.030.

Zou, H., Q.G. Zong, G.K. Parks, Z.Y. Pu, H.F. Chen, L. Xie, (2011), Response of high-energy protons of the inner radiation belt to large magnetic storms, J. Geophys. Res., 116, A10229, http://dx.doi.org/10.1029/2011JA016733

Source (Spectrum name) NMH* All SMH**	Number of points NMH All SMH	Av. dose rate (µGy h⁻¹) NMH All SMH	Experimental points description					
			Average orbit coordinates			Selecting requirements		
			Time	Long./Lat.(Deg.)/L value NMH SMH	Alt. (km)	Dose rate (µGy h⁻¹)/ Flux (cm⁻² s⁻¹)	L value/	D/F (nGy cm² part.⁻¹)
SEP All (Including SP)	286 1758 1434	629 529 1140	21/06-30/06/2015	(-83°, 50°)/3.8 (107°, -52°)/4.9	418	Dose>15		D/F>1.12
IRB	5876	335	21/06-30/06/2015	(-35.2°, -31.6°)/1.6	413	Dose>15		D/F>1.12
GCR	72,638	2.78	21/06-30/06/2015	(2.1°, 4.2°)/1.65	406	Dose<15		
ORB	2388 6101 3714	167 354 513	21/06-30/06/2015	(-101°, 49.4°)/3.52 (38.4°, -51.8°)/3.19	414	Flux>7		D/F<1.12
All sources	**41405 86400 44997**	**49 67.3 92.6**	**21/06-30/06/2015**	**(-7.4°, 32.3°)/1.73 (6.5°, -29.7°)/1.91**	**407**			
Additional table								
SEP	472 (334 in South mag. Hem.)	2,163	16:58-23:28 UT 22/06/2015	North Hem. (-78°, 50°) South Hem. (106°, -49°)	416	D>15		D/F>1.12
L>4 (GCR)	5003 (4666 in South mag. Hem.)	8.24	01/06-30/06/2015	North Hem. (-74°, 51°) South Hem. (130°, -50°)		Dose<15	L>4	
SP	1763 (1211 in South mag. Hem.)	18.02	21/03-10/06/2015	North Hem. (-85°, 49°) South Hem. (83°, -49°)	412	Dose>15	2.3<L<6	D/F>1.12
Pro	10	36,800	30/09/1999	Calibrations at cyclotron facility with protons of 7.8 MeV energy.				

*NMH means: North Magnetic Hemisphere (Dip latitude>0)
**SMH means: South Magnetic Hemisphere (Dip latitude<0)

Table 2. Statistics for the sources observed during the Expose-E/R/R2 missions

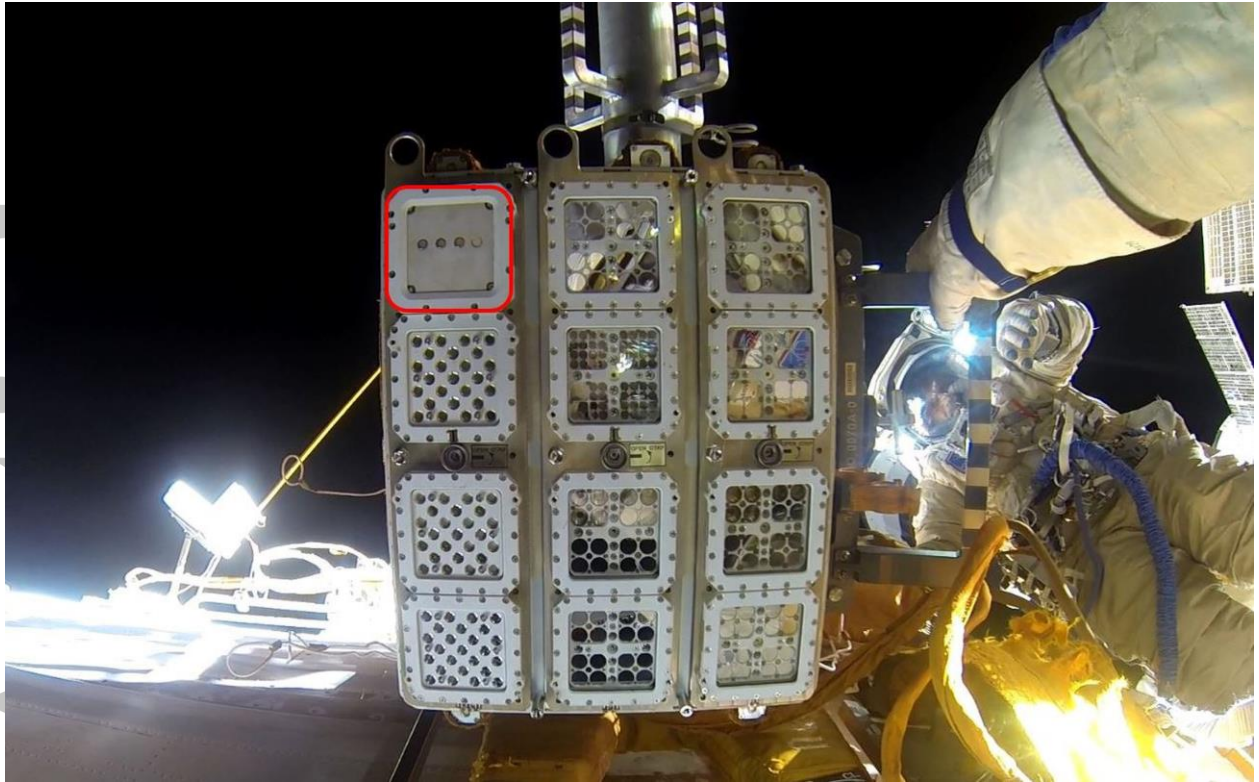| Source or dose limit	Min. value (μGy d^{-1})	Average absorbed daily dose rate (μGy d^{-1})	Max. value (μGy d^{-1})	Total accum. absorbed dose (Gy)	Assumed biological effective-ess Q	Calculated average equivalent daily dose rate (μSv d^{-1})	Total accum. equivalent dose for the Expose-R2 mission (Sv)	Total accum. equiv. dose for 30 days (Sv)	Total accum. equiv. dose for 365 days (Sv)
Measured by the R3D/E/R/**R2** instrument data				Assumed or calculated values using R3DR2 data					
GCR	76/79/**59**	91.1/81.4/**71.6**	102/90/**77**	0.0394 (394 days)/0.0233 (286 days)/**0.0318 (442 days)**	3.5	250.6	0.111	0.00752	0.0915
IRB	110/326/**340**	426/506/**567**	685/704/**844**	0.181 (425 days)/0.147 263 days/**0.251 (442 days)**	1.3	737.1	0.326	0.0221	0.269
ORB	0.25/0.64 **2.0**	8.64/89/**278**	212/2,348 **2,962**	0.0032 (432 days)/0.0229 (286 days)/ **0.123 (442 days)**	1.0	278	0.123	0.0083	0.101
SEP+SP **(only in R3DR2 data**	**0.64**	**9**	**2,848**	0.004 (442 days)	1.3	11.7	0.0052	0.00035	0.0043
Total				0.0224/0.191/**0.4098**			0.5652	0.03827	0.4658
Dose limits in LEO (NCRP, Report 132) Eye/Skin (Sv)								1.0/1.5	1.5/3

Fig. 1. External view of the R3DR2 instrument (in the left red square) as mounted on the EXPOSE-R2 facility. (Picture taken by Russian cosmonaut G. Pedalka (only his arm is seen in the upper-left corner, while cosmonaut M. Kornienko is seen in the left middle plane) on 15 August 2015 during an EVA to examine the EXPOSE-R2 facility outside the Russian "Zvezda" module.) (Picture credit ESA/RKA).
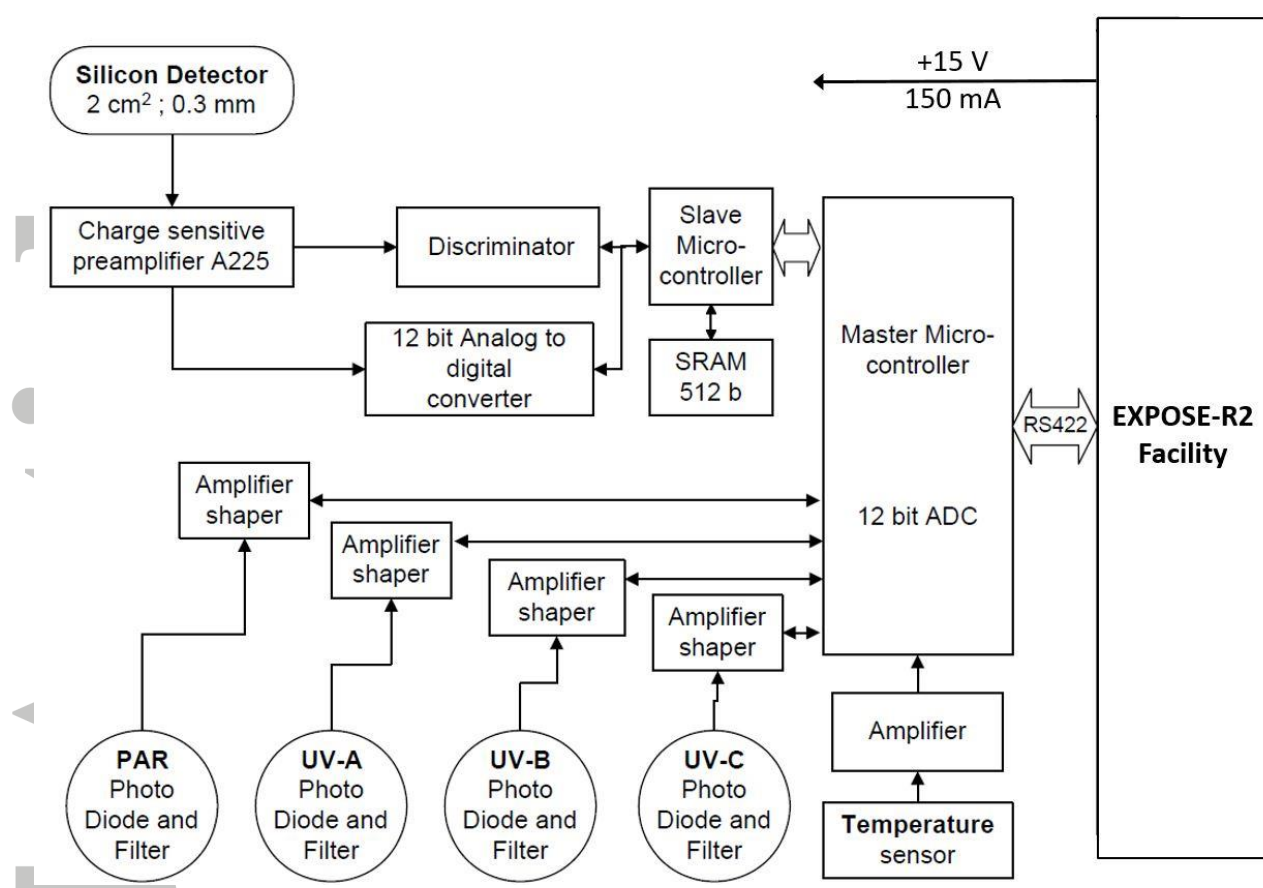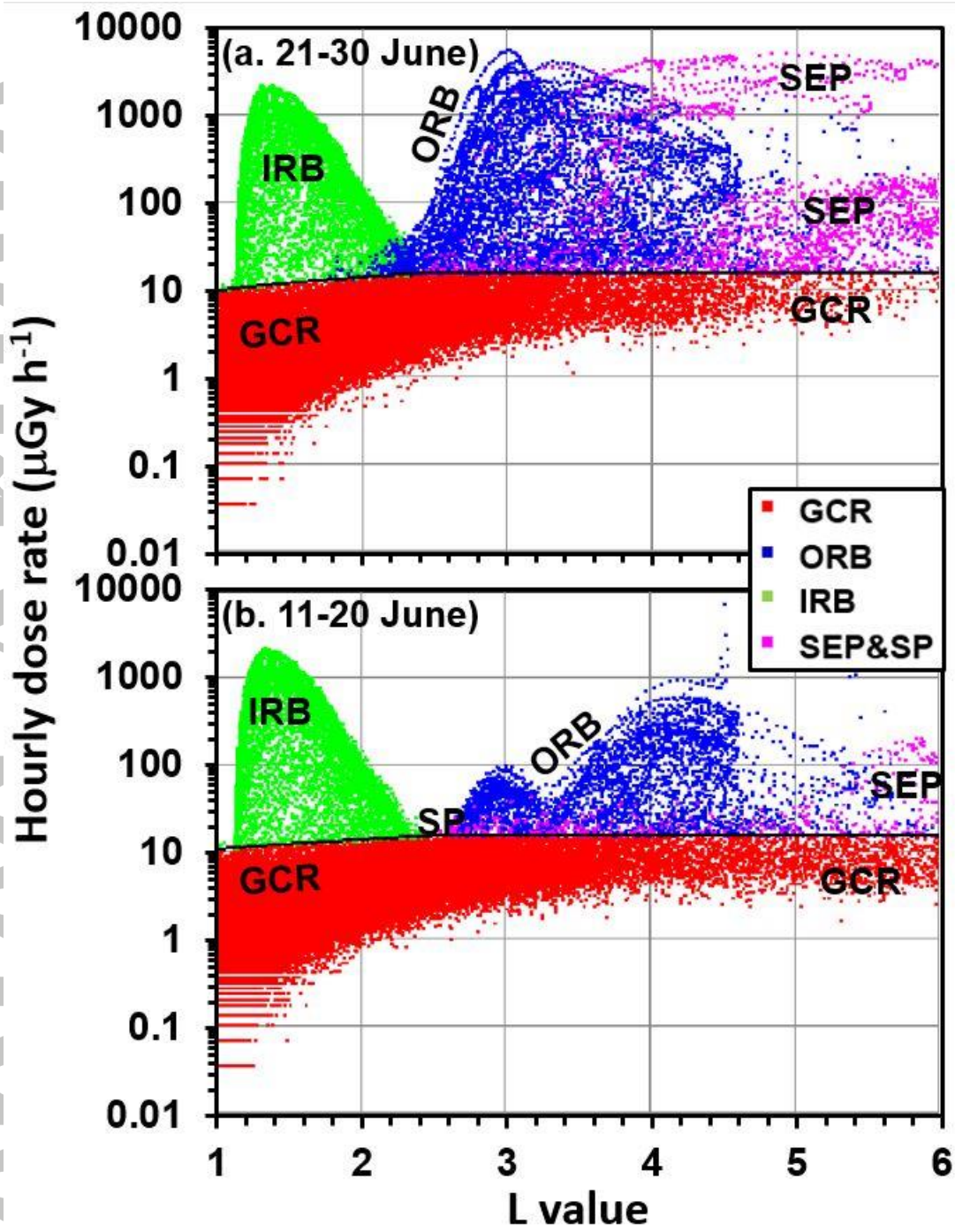
Fig. 2. Block diagram of the R3DR2 instrument.

Fig. 3. Latitudinal distribution of the dose rates measured with the R3DR2 instrument against McIlwain's L values for the period from the 11-20 and 21-30 June, 2015. Galactic cosmic rays (with dose rates typically < 15 μGy h^{-1}) are plotted with red points in the lower part of each figure. Green points in the upper left corner of the figure are associated with high-energy protons detected when the ISS crosses the SAA region of the IRB. They are characterized by dose rate >15 μGy h^{-1} and D/F > 1.12 nGy cm^2 particle^{-1}. The blue points in the center are associated with high-energy electrons in the ORB. They are characterized by dose rate >15 μGy h^{-1} and D/F < 1.12 nGy cm^2 particle^{-1} and flux >7 cm^{-2} s^{-1}. The magenta points that spread from the center toward the right side visualize the distribution of the SEP high-energy protons. Those magenta points with doses < 20 μGy h^{-1} are distinguished as secondary protons.
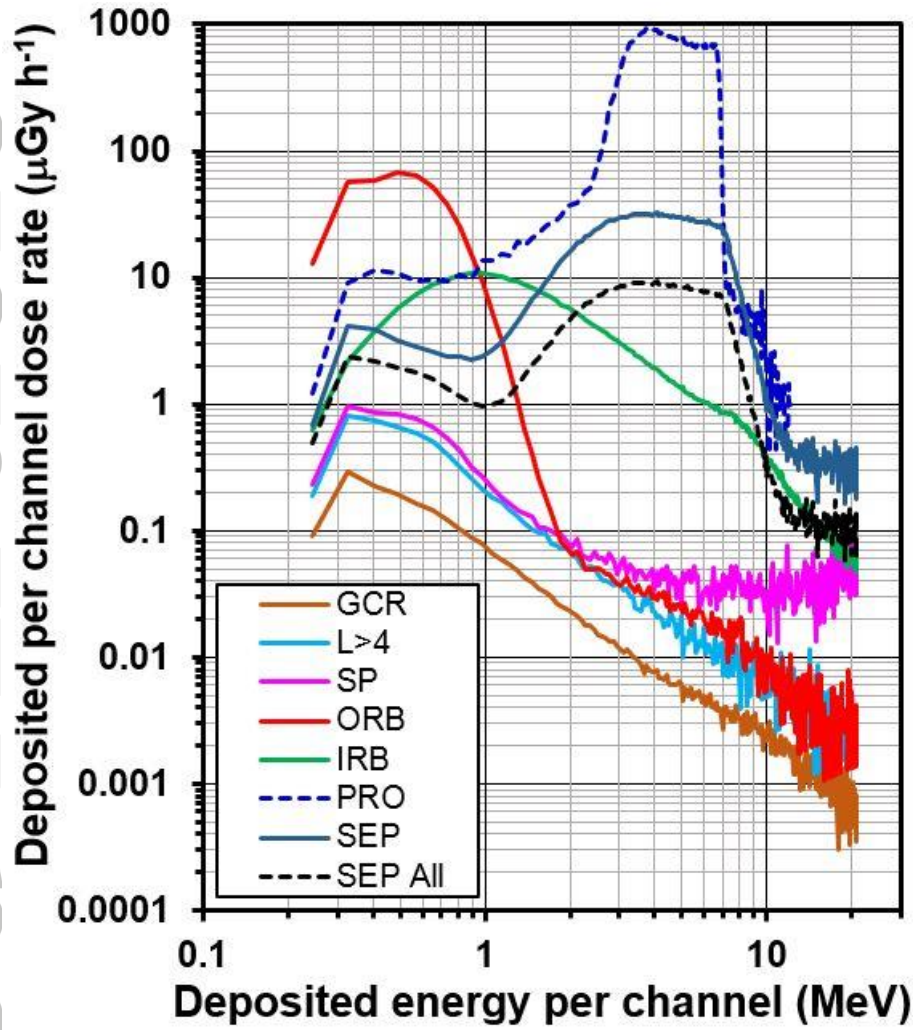
Fig. 4. Deposited energy spectra shapes for the period 21-30 June 2015. The PRO spectrum was obtained during the calibrations of Liulin DES type instruments.
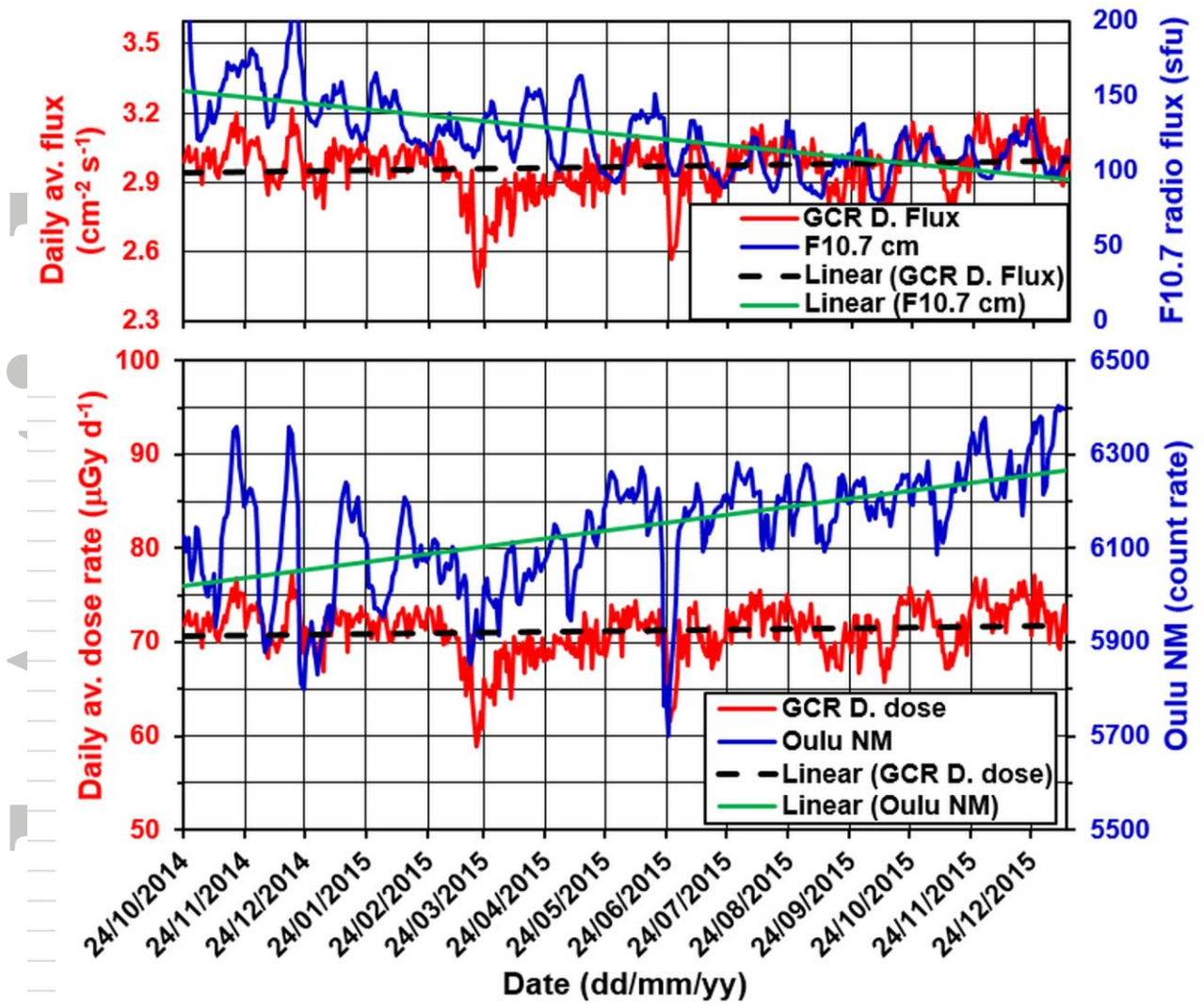
Fig. 5. Variations in the averaged GCR daily dose rates and flux during the period from 24 October 2014 – 11 January 2016.
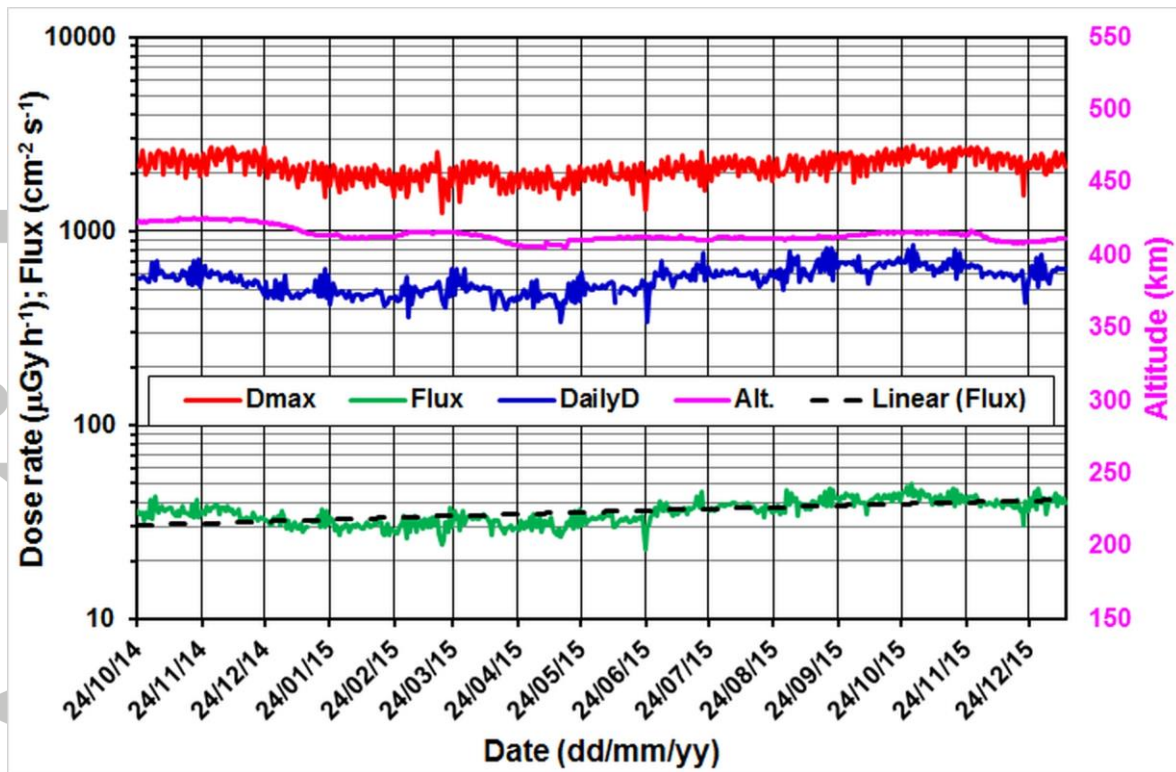
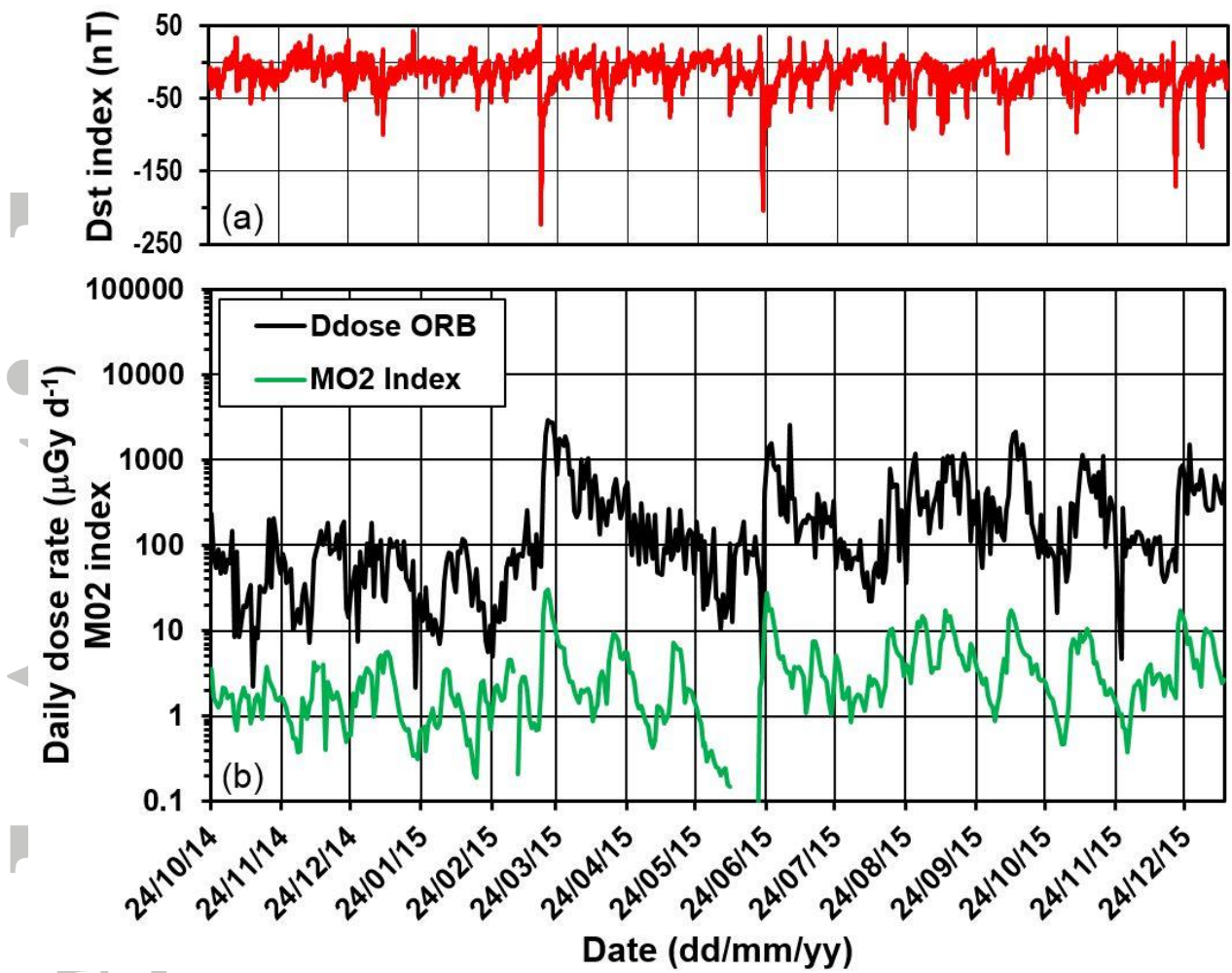Fig. 6. Variations of the IRB daily averaged dose rates and flux in the period from 24 October 2014 – 11 January 2016.

Fig. 7. Variations of the IRB daily averaged dose rates in the period from 24 October 2014 –
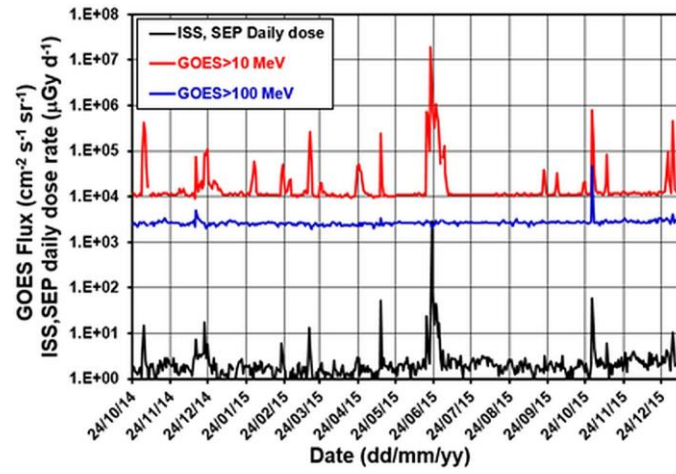11 January 2016.

Fig. 8. Variations of the SEP daily averaged dose rates in the period from 24 October 2014 – 11 January 2016.